# A Wide-Band Mechanically Stable Quasi-Optical Detector for 100—300 GHz

RYOJI KAWASAKI AND KAZUYUKI YAMAMOTO, MEMBER, IEEE

*Abstract*—**A wide-band mechanically stable quasi-optical detector for 100–300-GHz waves propagating in free space has been constructed. The circuit consists of a whisker diode and an oversized waveguide tuning section. The whisker diode using a honeycomb p–Si Schottky-barrier diode chip is placed on the aperture of the oversized waveguide open to the free space. For an incident power of 1 W/m$^2$, output voltage of 10–0.1 mV is obtained over the 100–300-GHz range. The present detector looks attractive for practical use in wide-band instrumentation.**

## I. Introduction

THE NEED for quasi-optical detectors in the millimeter waves and beyond has become apparent in many areas such as spectroscopy and radio astronomy. Several workers have constructed and reported quasi-optical detectors that are extensions of the conventional whisker diode structure commonly used in the microwave semiconductor devices [1], [2]. These detectors have a thin metallic wire (whisker) to obtain the coupling of applied radiation field to the diode structure. These types of detectors, however, usually have problems with respect to mechanical stability and handling ease due to the point contact configuration.

This paper presents a wide-band mechanically stable quasi-optical detector for 100–300-GHz waves propagating in the free space. In the present detector, a mechanically reinforced diode-mounting section is used which is designed to be demountable for easy handling. By using a honeycomb p–Si Shottky-barrier diode chip, the detector operates without any external dc bias source. This feature is useful in many practical applications. For an incident power of 1 W/m$^2$, the typical values of detector output voltage are 2.7 mV at 100 GHz, 0.6 mV at 180 GHz, and 0.22 mV at 260 GHz. In the following sections, the circuit structure, the measurement setup and the experimental results are described in detail.

## II. Circuit Description

A photograph of the detector constructed is shown in Fig. 1, which is an oversized waveguide mount with a whisker diode placed on the aperture of the guide open to the free space. The inside structure is shown in Fig. 2. The detector circuit consists of two major parts: 1) a diode-mounting section and 2) a tuning section.

Manuscript received April 28, 1978; revised November 10, 1978.

The authors are with Yokosuka Electrical Communication Laboratory, Nippon Telegraph and Telephone Public Corporation, 1-2356 Take, Yokosuka-shi, Kanagawa-Ken, 238-03 Japan.

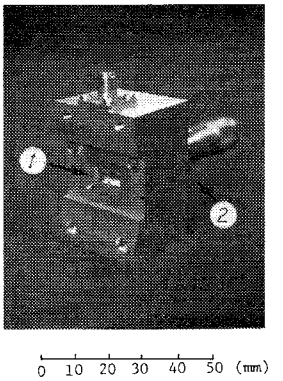


Fig. 1. Photograph of the quasi-optical detector. (1) A diode-mounting section; (2) a tuning section.

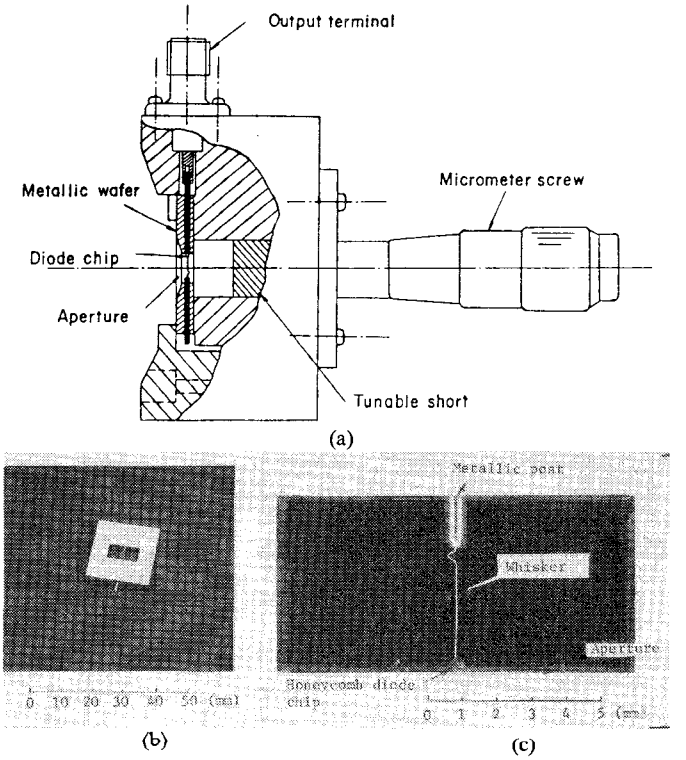


Fig. 2. Inside structure of the detector. A whisker diode is placed on the aperture of the metallic wafer. The metallic wafer is screwed to the oversized waveguide tuning section which has a short plane and a micrometer screw. The metallic post which supports the diode chip is insulated from the metallic wafer, and is connected to the center conductor of the coaxial output-terminal. (a) Inside structure of the complete detector. (b) A photograph of the metallic wafer. (c) Enlarged view of the aperture.

### A. Diode-Mounting Section

This section has a metallic wafer with a rectangular aperture of 10×5 mm, which is attached to the oversized

0018-9480/79/0500-0530$00.75 ©1979 IEEE

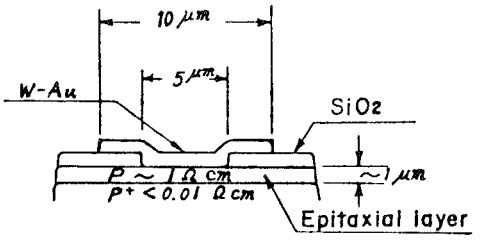


(a)

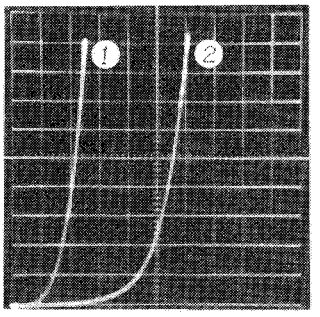


(b)

Fig. 3. Diode structure and $I$–$V$ characteristic. A p–Si Schottky-barrier diode is used [3]. 1) Forward characteristic (horizontal: 0.1 V/div., vertical: μA/div.); 2) backward characteristic (horizontal: 2.0 V/div., vertical: 10 μA/div.). (a) Diode structure. (b) $I$–$V$ characteristic.

waveguide tuning section as shown in Fig. 2. On the aperture of the metallic wafer, a p–Si Schottky-barrier diode chip with a honeycomb structure is placed. The junction diameter is 5 μm. The diode structure and the $I$–$V$ characteristic are shown in Fig. 3 [3]. The contact to the diode is made by pressing a spring-loaded whisker using a thin AuGa wire against one of the junctions on the surface of the oxide-protected diode chip. The whisker is 25 μm in diameter, and 3.3 mm in length. One end of the whisker is electrolytically sharpened to a tip radius of about 2 μm, and the other end is ultrasonically bonded to the top of the metallic post (0.6-mm diameter) which is supported by the metallic wafer. This construction yields a fairly good mechanical stability due to the fact that the whisker diode is protected by the rigid frame of the metallic wafer.

### *B. Tuning Section*

This section has an oversized waveguide of 16 mm ×8 mm and a tunable short. The short is moved by using a micrometer screw. Movable range of the short plane is 10 mm.

The detector circuit described above has the following properties:

1) the whisker provides the coupling of applied radiation field to the diode structure;
2) a wide-band detection is obtained by adjusting the tunable short;
3) the metallic wafer with a whisker diode is employed, and is demountable; therefore, the fabrication and handling of the whisker diode is easily performed;

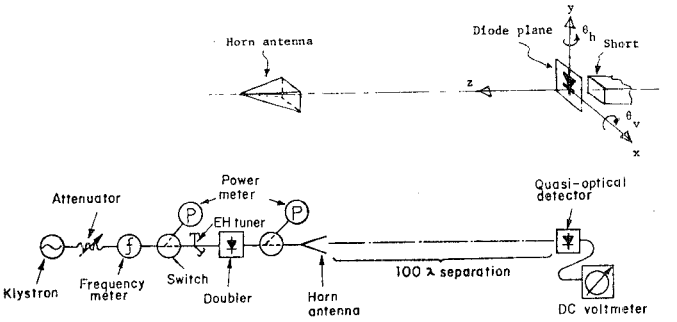


Fig. 4. Measuring setup. The 100–300-GHz wave propagating in the free space, radiated from the horn antenna, is detected by the quasi-optical detector which is screwed to a manipulator. $\theta_h$ and $\theta_v$ are the rotation around the $y$ and the $x$ axes, respectively.

4) a mechanically stable characteristic is obtained; the detectors reported here, have actually been in a stable operation for more than a year;
5) the barrier height of the p–Si Schottky-barrier diode employed is considerably lower than that of the GaAs diode usually used for submillimeter-wave detection; therefore, the detector circuit requires no bias source.

## III. Measurement Setup

The measurement setup used in the experiment is shown in Fig. 4. The transmitting equipment consists of a reflex klystron, a frequency doubler, waveguide components, and a horn antenna. The receiving equipment consists of the quasi-optical detector which is attached to a manipulator in order to adjust the horizontal and vertical direction of the detector, and a dc voltmeter with an input impedance of 10 MΩ connected directly to the detector output terminal.

The doubler has recently been constructed by our engineering group using a GaAs Schottky-barrier diode or a varactor diode with a junction diameter of 3–5 μm [4]. The waveguide components used are described in [5].

The detector is placed in the free space as shown in Fig. 4. The 100–300-GHz wave propagating in the free space, radiated from the horn antenna, is vertically polarized and not modulated. Let us denote $\theta_h$ and $\theta_v$ as the rotation angle around the $y$ and $x$ axes, respectively, as shown in Fig. 4. The following section describes the performance for an incident power per unit area.

## IV. Performance

### *A. Output Voltage Versus Incident Power Density*

The measured output voltage versus incident power density characteristics for $\theta_h = \theta_v = 0°$ are shown in Fig. 5. The data points are obtained by adjusting the tunable short for optimum sensitivity at each power level.

The measured points plotted are in alignment with the line drawn in the figure which shows the square-law detection characteristics. When it is supposed that the incident power to the aperture of the metallic wafer is completely supplied to the diode circuit, the input power to the diode circuit is equal to $P_i \cdot A$ ($P_i$ is the incident

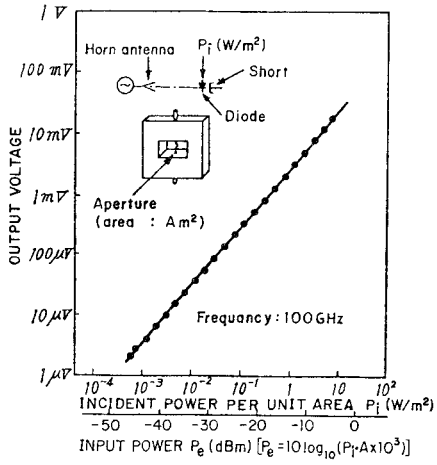


Fig. 5. Output voltage versus incident power per unit area. The measured points plotted is in alignment with the line drawed in the figure, which shows the square-law detection. The data points are obtained by adjusting the tunable short for optimum sensitivity at each power level.

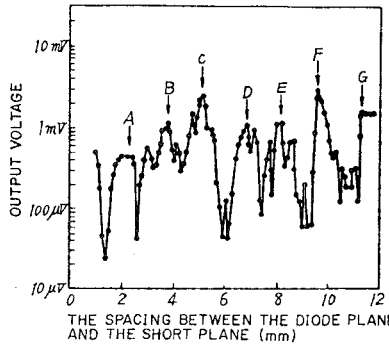


Fig. 6. Output voltage versus the spacing between the diode plane and the short plane. The spacing of $(2n+1)\cdot(\lambda/4)$ ($\lambda$ is the wavelength in the free space and $n$ is the zero or positive integers) gives one of the peaks of output voltage, (frequency: 100 GHz, incident power: 1 W/m$^2$).

power per unit area, and $A$ is the area of the aperture) which is shown on the horizontal axis. We can see the sensitivity expressed by output voltage ($V$) per input power (dBm).

### B. Tuning Effect

Output voltage versus the spacing between the diode plane and the short plane for $\theta_h = \theta_v = 0°$ is shown in Fig. 6. Several peaks of output voltage are observed over the movable range of the short plane. These peaks, which are marked with $A$–$G$, are arranged with an equal distance of about $\lambda/2$ (1.5 mm at 100 GHz), as shown in Table I. The spacing of $(2n+1)\cdot(\lambda/4)$ ($\lambda$ is the wavelength in the free space, $n$ is the zero or positive integers) gives one of the peaks of output voltage.

### C. Field Patterns of Detection

Horizontal and vertical patterns of detection are shown in Fig. 7. Horizontal field pattern of Fig. 7(a) is approximately symmetrical with respect to the axis of $\theta_h = 0°$. A pair of side robes are observed at about $\theta_h = 22°$. The

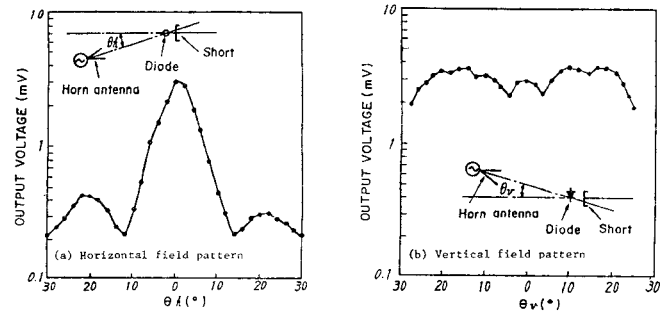


Fig. 7. Field patterns of detection. $\theta_h$ and $\theta_v$ are the rotation around the $y$ and $x$ axes, respectively, as shown in Fig. 4. The data points are obtained by adjusting the tunable short for optimum sensitivity at each angle, (frequency: 100 GHz, incident power: 1 W/m$^2$).

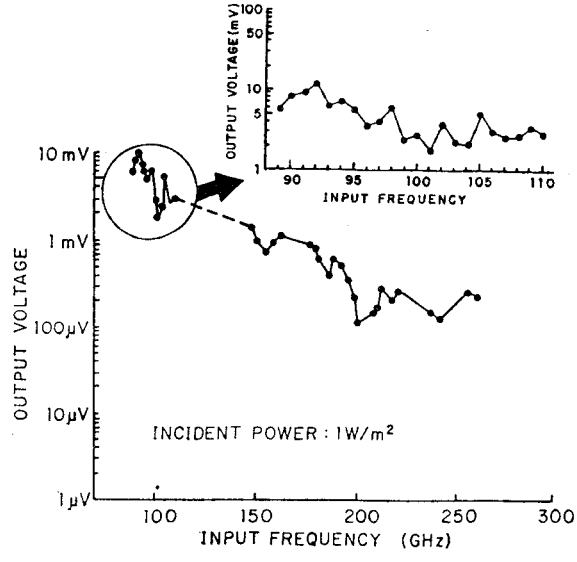


Fig. 8. Output voltage versus input frequency. Wide-band data over the short millimeter-wavelengths region and detailed data around 100 GHz measured with a distance of 1 GHz are shown. The data points are obtained by adjusting the tunable short for optimum sensitivity at each frequency.

TABLE I
DISTANCE BETWEEN THE PEAKS OF THE OUTPUT VOLTAGE SHOWN IN FIG. 6.

| | |
|---|---|
| A–B : 1.5 mm<br>B–C : 1.3 mm<br>C–D : 1.7 mm<br>D–E : 1.4 mm<br>E–F : 1.45 mm<br>F–G : 1.7 mm | average : 1.51 mm |

vertical field pattern of Fig. 7(b) gives a pair of a little higher level of the output voltage at about $\theta_v = 10°$–$20°$. The field patterns presented above is useful in alignment or circuit design of the detector.

### D. Output Voltage versus Input Frequency

The output voltage versus input frequency characteristics for $\theta_h = \theta_v = 0°$ are shown in Fig. 8. In this measurement, the detector circuit is tuned for optimum sensitivity

at each frequency. Wide-band data over the short millimeter-wavelengths region, and detailed data around 100 GHz measured with a distance of 1 GHz are given in the figure. These data show the following: 1) wide-band detection over the 100–300-GHz region is obtained, and detection up to the submillimeter-wavelengths region can be expected; and 2) movable shorts employed are effective for wide-band tuning.

## V. Conclusion

Circuit structure and performance of a wide band and mechanically stable quasi-optical detector for 100–300 GHz is discussed. The detector reported here is convenient for applications such as spectroscopy and radio astronomy over the short millimeter-wavelengths region. Moreover, this circuit technique is easily extended to submillimeter detection and mixing.

## Acknowledgment

The authors wish to thank Dr. H. Kimura, Dr. M. Fujimoto, and Dr. M. Akaike for their valuable guidance and discussions.

## References

[1] L. M. Matarrese and K. M. Evenson, "Improved coupling to infrared whisker diodes by use of antenna theory," *Appl. Phys. Lett.*, vol. 17, no. 1, p. 1, July 1970.
[2] K. Mizuno *et al.*, "Submillimeter detection using a Shottky diode with a long-wire antenna," *Appl. Phys. Lett.*, vol. 26, no. 11, p. 1, pp. 605–607, June 1975.
[3] S. Yuki *et al.*, "Millimeter-wave impatt oscillators and wideband detectors," *Tech. Group Microwaves, Inst. Electron. Commun. Eng. Japan*, vol. MW-75-58, Sept. 1975.
[4] H. Kato *et al.*, "A 200-GHz-output doubler," in *Proc. 1977 Nat. Conv. Inst. Electron. Commun. Eng. Japan*, vol. 3, p. 180, Mar. 1977.
[5] K. Yamamoto *et al.*, "200-GHz waveguide components," *Tech. Group on Electron. Measurements, Inst. Elect. Eng. Japan*, vol. EM-77-20, June 1977.

# An Avalanching Optoelectronic Microwave Switch

RICHARD A. KIEHL, MEMBER, IEEE

***Abstract*—A new optoelectronic microwave switching device is described. The device is composed of a semiconductor junction diode that is incorporated into a transmission line and illuminated with optical pulses from a semiconductor laser. Switching of microwave signals is achieved by changes in the RF impedance of the diode's high-field region resulting from an optically induced switching between low- and high-level avalanche states.**

**Experimental results demonstrating the switching characteristics and speed of this device are presented along with a basic theory of operation. The ultimate capabilities of this device and its advantages over conventional p-i-n diode switches and other optoelectronic switching devices are also discussed.**

## I. Introduction

THERE HAS BEEN recent interest in the use of optical techniques for the control of microwave signals. This interest has been stimulated by the need for faster switching of moderate- to high-power microwave signals for both high-speed digital microwaves and high-resolution radar systems. For such applications, optical techniques offer higher speeds than conventional diode-switching techniques (p-i-n diodes), which are hampered by basic power-speed limitations [1]. In addition, optical control techniques permit virtually complete isolation between the RF and modulator circuitry of a system, thus eliminating both the problem of spurious "modulation-circuit oscillation" of the RF source, and of radar desensitization due to RF leakage.

Two basic approaches for optical control of microwave signals are being investigated. The first is direct control [2]–[4] of the internal dynamics of a solid-state oscillator. In this approach, optical signals are used to generate free carriers within the active region of, for example, a TRAPATT diode oscillator. Control of the frequency and amplitude of the oscillations is achieved through the modification of the diode's oscillatory dynamics caused by the presence of these optically generated carriers. Similarly, optical control of the gain characteristics of solid-state amplifiers is also expected to be possible.

In the second approach, which has been followed in the work described here, the optical signal is used to control the RF impedance of an element placed in the microwave

Manuscript received May 12, 1978; revised October 30, 1978. This work was supported by the United States Department of Energy (DOE) under Contract AT(29-1)789.

The author is with Sandia Laboratories, Albuquerque, NM 87185. Sandia Laboratories is a United States Department of Energy Facility.

0018-9480/79/0500-0533$00.75 ©1979 IEEE